2020-06-04

Comprehensive characterization of elastomeric Polyhydroxyalkanoate and its sensor applications

Goran Stojanović, Jasmina Nikodinović-Runić, Stefan Švenderman, Tijana Kojić, Milan Radovanović, Momir Mikov, Danijela Ranđelović

Elsevier

Goran Stojanović, Jasmina Nikodinović-Runić, Stefan Švenderman, Tijana Kojić, Milan Radovanović, et al. 2020. Comprehensive characterization of elastomeric Polyhydroxyalkanoate and its sensor applications. Materials Science & Engineering C 115. doi: https:// doi.org/10.1016/j.msec.2020.111091.

https://open.uns.ac.rs/handle/123456789/16300

Title page:

Comprehensive characterization of elastomeric Polyhydroxyalkanoate and its sensor applications

Goran Stojanović[a], Jasmina Nikodinović-Runić[b], Stefan Švenderman[a], Tijana Kojić[a,*], Milan Radovanović[a], Momir Mikov[c], Danijela Ranđelović[d]

[a]Faculty of Technical Sciences, University of Novi Sad, Trg Dositeja Obradovića 6, 21000 Novi Sad, Serbia
[b]Institute of Molecular Genetics and Genetic Engineering, University of Belgrade, Vojvode Stepe 444a, 11000 Belgrade, Serbia
[c]Faculty of Medicine, University of Novi Sad, Hajduk Veljkova 3, 21000 Novi Sad, Serbia
[d]Department of Microelectronic Technologies, Institute of Chemistry, Technology and Metallurgy, University of Belgrade, Njegoševa 12, 11000 Belgrade, Serbia

1. Introduction

More than 320 million tons of plastics generated per year represent a serious environmental problem and potential hazard [1]. Biopolymers, particularly polyhydroxyalkanoates (PHAs), are promising alternatives to a slow- or nondegradable petroleum-based plastics [2]. PHAs are biopolyesters that have been applied in many sectors of modern science and industry. PHAs are biocompatible and biodegradable and as such have a positive social and environmental dimension [3]. Degradation metabolites of PHAs are not toxic; they degrade into carbon dioxide and water (under aerobic conditions), or carbon dioxide and methane (under anaerobic conditions) [4]. In 2007, the Food and Drug Administration (FDA) approved the use of P(4HB) for surgical sutures in clinical applications and from that period medical applications of PHAs have increased [5]. Examples of these applications include: scaffold for heart valve and cartilage tissue, micro- and nanospheres and antibacterial coating material [6], [7]. PHAs are mainly produced by biotechnological (fermentative) methods. More than 150 PHA subunits have been identified to date [8] and their structure determines mechanical properties and degradation rate [9]. PHAs can be degraded by the activity of microorganisms (bacteria and fungi), but also by enzymes in bovine serum, pancreatin and synthetic gastric juice [10]. The carbon sources and the metabolic potential of the microorganisms involved in their synthesis have an influence on PHA chemical properties [11]. The molecular mass of PHA is dependent on growth conditions such as carbon source, culture medium or fermentation mode [12]. PHAs are insoluble in water, but soluble in chloroform and demonstrated a good resistance to moisture and UV light [13]. The composition of the monomeric unit of PHAs has an influence on their mechanical and temperature characteristics with short chain length (scl) PHAs being hard, brittle polymers while medium chain length (mcl) PHAs are softer, more elastomeric polymers [14]. The mechanical properties of PHAs can be improved by means of an electrospinning technique [15]. Combining PHAs with other polymers can improve their flexibility, which is an important parameter for medical applications [16]. The melting temperature of scl-PHA is above 140ºC, while melting temperatures of mcl-PHA is usually between 40 and 60ºC, and above this range they are amorphous and sticky. However, melting temperatures are highly dependent on the monomer composition, thus mcl-PHA homopolymers can have melting temperatures even higher than 60ºC [16, 17]. The applications of PHAs as biodegradable polymers is manifold and it will be even higher if their mechanical and hydrophobic properties can be modified and fine-tuned with respect to the requirements of the specific application [18]. Aligning fibers in the internal structure of PHA, achieved by the electrospinning technique, can improve the mechanical characteristics compared with randomly oriented fibers inside the PHA structure [19]. Furthermore, the wettability and the contact angle of polyhydroxyalkanoates electrospun membranes can also be adjusted by changing the polymer concentration [20].

An analysis of the literature reveals that the majority of published papers have considered (bio)medical applications of PHAs, but there is a lack of articles reporting sensor applications of PHAs. Previously, PHB film was reported to be suitable as a membrane for the incorporation of haemoglobin to boost the electron transfer rate of this protein. Further modifications using pyrolytic graphite electrodes and/or the addition of peroxidises paved the way towards the application of PHB-embedded proteins as an integral part of H_2O_2 biosensors [21], [22]. Only one more biosensor application was found in the literature; another type of PHA (biopolymer containing 3-hydroxyvalerate (3HV), 5-hydroxydecenoate (5HDE) and 3-hydroxyoctadecenoate (3HODE)) was used to develop of a hybrid nanocomposite based biosensor containing gold nanoparticles, horse radish peroxidase and PHA/AuNP/HRP/ITO for the quantitative detection of artemisinin in body fluids [23].

This study aims to expand the application niche of PHA based sensors. Herein we analyse the structural, morphological and mechanical properties of a biotechnologically produced PHA sample, more specifically a medium chain length PHA (mcl-PHA). The inductive-capacitive (LC) resonant circuit structure was constructed using this sample. This device was applied for the remote detection of liquid solution in which the sensor was immersed (such as artificial saliva or simulated gastric fluid). Using

the principles of wireless coupling we have successfully detected the chosen fluid by measuring the shift in the resonant frequency of the LC structure fabricated on a PHA substrate covered with gold as a conductive material.

2. Materials and Methods

2.1 Production method of PHA sample

Mcl-PHA biopolymer, specifically polyhydroxyoctanoate (PHO; contained > 95% 3-hydroxyoctanoic acid as the monomer), was produced via fermentation using Pseudomonas putida KT2440 strain by Bioplastech Ltd., using basic fermentation conditions as described previously [24] and the octanoic acid as substrate [25]. The PHO content of cells was determined by methanolysis of 10 to 15 mg of lyophilized cells in the presence of 15% (vol/vol) sulfuric acid. The resulting methyl esters of the constituent hydroxyalkanoic acids were analyzed by gas chromatography. For identification of the methylesters, gas chromatography-tandem mass spectrometry (GC-MS-MS) was also performed. The remaining monomers were trace amounts of 3-hydroxyhexanoate and 3-hydroxydecanoate. Mcl-PHA films were prepared by the solvent casting method. Initially, PHA (2 g) was dissolved in acetone (10 mL) at 25 ºC, after which it was poured into a glass Petri dish and left to dry in the air at ambient temperature for 10 days.

2.2 Characterization methods

A 3D optical Profilometer (Huvitz microscope with Panasis software) and scanning electron microscopy (SEM, Hitachi TM3030) were used for structural and surface analysis. Morphology, roughness and frictional properties of the sample were studied with an atomic force microscope AutoProbe CP-Research SPM (TM Microscopes-Bruker) using a 90 μm large area scanner. The measurements were performed in contact mode using Bruker Phosphorous (n)-doped silicon contact metrology probes, model MPP-31123-10 with Al reflective coating and symmetric tip. AFM images of topography, “error signal” and Lateral Force Microscopy (LFM) signal were taken and later analyzed using two software packages, Image Processing and Data Analysis Version 2.1.15 and SPMLab Analysis, DI SPMLab NT Ver. 6.0.2. The contact angle method was used for wettability analysis. The contact angle measurement was performed in an optical laboratory located in a clean room class ISO 8, nitrogen and air class ISO 5, vacuum. A Bausch & Lomb MicroZoom Microscope connected to a laptop with software tool ISCapture were used for photography. Laboratory Power Supply Manson NSP 3630 provided the necessary light for measurement. For mechanical characterization, a nanoindentation method was used with a G200 nanoindenter, having a Berkovich diamond tip. A Vector Network Analyzer E5071B was used for measuring S-parameters of LC structure, in different media.

2.3 Preparation of test fluids

Two different fluids were prepared in order to test functionality of the fabricated structure: (a) artificial saliva and (b) simulated gastric fluid. The artificial saliva had the following composition: Sodium carboxymethylcellulose – 10 g/l, Sorbitol – 29.95 g/l, Methyl p-hydroxybenzoate – 1.00 g/l, Sodium chloride – 0.87 g/l, Di-potassium hydrogen orthophosphate – 0.80 g/l, Potassium chloride – 0.22 g/l and Lemon aroma – 5 ml. The simulated gastric fluid, without pepsin, was prepared as mixture of 0.2% (w/v) Sodium Chloride in 0.7% (v/v) Hydrochloric Acid adjusted to pH equal to 1.2 [26].

3. Results and Discussion

3.1 Structural, morphological and wettability properties of PHA sample

3.1.1. Structural characterization

In the last few years, PHAs have been studied to be used in tissue engineering for hard and soft tissue replacement, and as therapeutic delivery carriers [27]. For such applications mostly scl-PHAs, such as polyhydroxybutyrate (PHB) and its copolymers have been applied.

In this study, polyhydroxyoctanoate (PHO), representative of the mcl-PHA family, was evaluated for biosensor applications due to its specific thermo-elastomeric characteristics. Processed mcl-PHA film sample is shown in Fig. 1(a). Structural characterization was performed by SEM to visualise the surface and the cross section of the PHA sample. An SEM micrograph of the polymer surface with a magnification of 200 is presented in Fig. 1(b), while a cross section of the sample with magnification of 250 times is depicted in Fig. 1(c). Speckles of dust are evident on the surface of the film (Fig. 1(b)) while the side of the film that was in contact with glass during the solvent casting appears denser, as the cross section revealed (Fig. 1(c)).

Figure 1.

A 3D Optical profilometer was used to determine the exact thickness of the PHA polymer. The role of the profilometer was to provide 2D and 3D insight into topographic surfaces, and was used for micro- and nano-level measurements. Due to the transparency of the sample, the surface of the polymer was coloured purple with a marker, prior to starting measurement with the 3D Profilometer. The purple dye did not affect the measurement parameters or the performance of the device. The 2D image obtained is presented in Fig. 2(a) with magnification of ×20, and the 3D image is presented in Fig. 2(b). The 3D profile shows the thickness of the sample, which was estimated to be around 300 μm. The polymer was not of uniform thickness across the whole surface, and varied in the range ± 10 μm.

Figure 2.

3.1.2. Morphological characterization

Selected results of AFM characterization are presented in Figs. 3 and 4. The 3D topography of the sample is shown in Fig. 3 for the two scanning areas, (a) 50 μm × 50 μm, and (b) 5 μm × 5 μm. For these areas, RMS roughness of the sample was 608 nm and 73 nm, respectively. Results of LFM measurements are shown in Fig. 4. For the mentioned scanning areas, topography and LFM images are shown in parallel. By analyzing these images we can conclude that the sample surface is heterogeneous regarding frictional properties. The darker the region on the LFM image, the higher the value of the friction coefficient. In other words, the darker regions are “stickier” than the rest of the sample.

Figure 3.

Figure 4.

PHA films or membranes can be produced by various techniques that include compression-molding, solvent-casting, or electrospinning, and more recently 3D printing fabrication [28]. It has been shown previously that solvent-casted films have higher roughness in comparison to the compression-molded PHA membranes, however that did not affect the adherence of cerebellar granule neurons [29].

3.1.3. Characterization of wettability

For this purpose, we used the contact angle method where the static contact angle of a droplet on a polymer was measured over a period of time until the droplet (about 2 μl) was absorbed or spilled over the surface. The droplet images were analyzed by ImageJ software (option drop_analysis) depicted in Fig. 5.

Figure 5.

Fig. 5(b) illustrates the change of contact angle for a drop of distilled water over a period of 10 minutes. The values of the contact angle over the entire measurement period, to which the polymer was subjected, are below 90°, which categorize this polymer as hydrophilic, which means with higher wettability. An increase in the number of polar groups can make polymers more hydrophilic. This property is favorable for PHA sensor applications such as the LC sensor described in this paper, because it ensures that the liquid medium has better contact with the substrate.

3.2 Mechanical properties of PHA sample

One of the most important material properties is its mechanical endurance, which shows how much load (force, moment) a structure fabricated of the specific material can resist. Multiple nanoindentation tests were carried out with sets of ten indentations to ensure the credibility of the measured results. A preset depth of 5 μm was set, while the reaching load time was set to 15 s, and the peak loading time was set to 5 s. Nanoindentation testing was performed in three cases: (1) PHA sample; (2) PHA sample after incubation in artificial saliva for twenty-four hours, and (3) PHA sample after immersing in a simulated gastric fluid for twenty-four hours. The results obtained are depicted in Fig. 6.

Figure 6.

Fig. 6 shows the mean load–displacement curves for a maximum preset depth of 5 μm, where the penetration loads were around 2.7 mN for pure PHA, 2.5 mN for the polymer in saliva, and 2 mN for the polymer in gastric acid. It can be seen from Fig. 6 that the displacement into the surface exceeds the preset depth of 5 μm by a few nanometers, due to the hold time of 5 s on the preset depth so the tip enters a few nanometers more into the studied material. The obtained results confirmed theoretical expectations; the pure polymer demonstrated the highest resistance to mechanical stress. When the polymer was in saliva, this fluid reduced its mechanical properties, softening the material. The polymer that was immersed in the gastric fluid exhibited the lowest resistance to mechanical force. This is due to gastric fluid being an acid with pH around 1.2, which leads to degradation of the polymer and the breaking of double bonds within the polymer structure. The measured values of Young's modulus were 58.8 MPa in the case of pure PHA sample, 49.1 MPa for PHA in the artificial saliva and 38.1 MPa for PHA in the gastric fluid, respectively. The hardness value was 8 MPa for the PHA sample, 7 MPa for PHA in the artificial saliva and 5 MPa for PHA in the gastric fluid. These differences in elastic modulus and hardness values are a consequence of the exposure of the PHA sample to fluids that affected its elasticity and strength. The obtained values of the studied parameters are in good agreement with the data available in the literature. In [30] Young's modulus had a maximum of 25.4, 14.1, and 12.6 MPa for polyhydroxyoctanoate (PHO) films obtained from ethyl acetate, acetone, and chloroform solution, respectively. These values are comparable with the values for Young's modulus presented in our study, however, in [30], authors used an additional step for PHO film purification, which is one of the reason to consider our approach more eco-friendly. In our study, the ratio "displacement/thickness of the PHA film" was very low (around 0.016), meaning that nanoindentation tip will reach only the superficial layer of PHA. However, a thinner polymer film will have higher Young's modulus values, more precisely higher values of displacement/thickness ratio will result in an increase of Young's modulus, which is caused by the substrate effect.

Since the sensor proved to be a fully functional device, several material characterization methods were applied in order to assess the quality of the solvent-casted mcl-PHA film itself as well as to analyse structural, morphological, mechanical and wettability properties, which are essential for the underlying operation principle and field of application of the sensor. SEM analysis was used to detect density of the polymer as a substrate of the developed sensor. 3D profilometer was used to determine the thickness of the substrate, because sensor properties are dependent on this thickness. AFM analysis was implemented to determine the roughness of used PHA film, because this surface property influences how applied material or media will have a good adherence on the surface of the structure. Most biosensor applications for PHA polymers would be within a liquid environment, thus wettability was also studied. One of the intended applications of the proposed structure is in the field of the self-degradable sensors in the media in our body. Because of that, we also analyzed mechanical properties or how the presented sensor softens up when exposed to saliva or gastric fluid.

3.3 Sensor applications

We designed an inductor-capacitor (LC) structure, composed of an interdigitated capacitor with 5 pairs of fingers (electrodes) and a helically wound inductor. Uniquely, both parts (components) are planar and realized in one layer, which means there is no overpass or underpass such as would usually be used in spiral inductor design. The width of the electrodes and the gap between them were both equal to 600 μm. The total dimension of the LC structure was 30 mm × 12 mm. The LC sensor was fabricated using a cutting plotter machine, curving the structure in the PHA substrate (Fig. 7(a)). After that, gold was vapored onto this structure, as can be seen in Fig. 7(b), in order to obtain the conductive structure at the top. Nominal capacitance of the inderdigitated part of the structure was around 10.76 pF, whereas the inductance of the inductive part of the structure was approximately 1.53 nH.

Figure 7.

The Vector Network Analyzer (VNA) was used to measure the electrical characteristics of the sensor as it is depicted in Fig. 8, using a copper antenna coil.

Figure 8.

The S11-parameter of the antenna was measured using VNA and it was subtracted from the measured value of the S11-parameter obtained for the PHA-based LC structure exposed to different media. This eliminated any error introduced by the antenna itself. The first measurement was conducted under conditions such that the air was the dielectric material between the fingers of the interdigitated capacitor. The second and third measurement cycles were performed with artificial saliva or artificial gastric fluid, respectively, between the electrodes of the capacitor. The measured amplitude of the S11-parameter as a function of frequency is presented in Fig. 9, for the three above-mentioned media.

Figure 9.

It can be concluded from Fig. 9, that not only a shift in the resonant frequency was obtained when the sensor was exposed to different media, but also the magnitude of the S11 parameter increased in the liquid medium. The sensitivity of the proposed sensors can be expressed by $\Delta S_{11}/\Delta f_{res}$ and the value of 0.3 dB/MHz was obtained. Figure 10 demonstrates a shift in the resonant frequency of LC structure towards lower values. The value and change in the resonant frequency is determined by the type of dielectric located between the fingers of the interdigitated capacitor of the LC resonant circuit structure. Depending on the value of the relative permittivity of the material placed between the capacitor

electrodes, the capacitance of the capacitor in the LC structure varies. Capacitance has the lowest value in air while it increases after exposure to the artificial saliva, and even more after immersion in the artificial stomach acid. The resonant frequency is inversely proportional to this capacitance, based on the equation $f_{res} = 1/2 \cdot \pi \sqrt{L \cdot C}$. The studied media, artificial saliva and simulated gastric juice, have some similarities (containing water, mucus, salt), but also some differences (presence of iodide, pertechnetate, and bromide). These differences lead to different values of their relative permittivity. The difference in the dielectric constant was used to change capacitance of the capacitive part of the proposed sensor structure and consequently its resonant frequency. By means of the antenna coil, this shift in the resonant frequency can be monitored remotely, without contamination of the analysed media. Measuring S-parameters, using Vector Network Analyzer E5071B, we can determine both amplitude of S11-parameter and f_{res} in different media. This instrument was chosen as it enabled application of wireless (using antenna) and non-contact measuring principles. The qualitative advantages of this approach are as follows: (a) the terminals (wires) are not necessary from the component under test; (b) the contamination effects are eliminated; (c) the applied method is non-destructive for the tested component.

Figure 10.

Figs. 9 and 10 demonstrate that the highest resonant frequency value of the studied PHA-based LC structure was reached in air, being equal to 1.24 GHz. Resonant frequency drops to 1.23 GHz when the artificial saliva was used as the dielectric. The lowest value of the resonant frequency in the LC structure was observed when artificial gastric fluid was used as the dielectric, being equal to 1.22 GHz. Thus, a shift in the resonant frequency of 10 MHz per new medium was obtained, which can be also used as a measurable indicator of the sensitivity of the proposed structure. To compare the sensitivity of the proposed PHA-based sensor and other type of sensors from literature that also used resonant frequency as a measured quantity, Table 1 summarizes a comparison among different studies dealing with sensors for detection of various parameters of the human body. From Table 1, quantitative benefits of the proposed technique can be also noticed, because the difference in S11 amplitude and shift of resonant frequency between the various media has high values (1 dB/5 dB and 10 MHz, respectively), which enables clear distinction between them.

Table 1

Comparison of the sensitivity of sensors proposed in this paper and other reported studies.

Paper	Detection parameter	Sensing principle	Sensitivity (shift in)	
			Resonant freq.	Amplitude |S11|
This work	saliva, gastric fluid	wireless LC	10 MHz per new medium	1 dB for saliva 5 dB for gastric fl.
Ref. [31]	gastric pressure	inductive coupling LC	0.6 kHz / mmHg	n.a.
Ref. [32]	pH of liquid sample	planar inductor	4 MHz / pH	n.a.
Ref. [33]	glucose, galactose, fructose	capacitive coupling split rings	304 kHz, 540 kHz, 2.2 MHz / mg/dl	0.01, 0.0125, 0.0075 dB / mg/dl
Ref. [34]	pH of liquid sample, such as gastric acid	capacitive sensor + VCO	0.35 MHz / pH	n.a.
Ref. [35]	ε_r value (for saliva sample)	coplanar interdigital capacitor	129 MHz for ε_r from 60 to 70	n.a.
Ref. [36]	glucose concentration in fluid	liquid channel-loaded capacitor	2 MHz / mg/ml	n.a.
Ref. [37]	aqueous glucose concentration	microwave dielectric resonator	n.a.	1.2 dB from water to glucose conc. of 300 mg/ml

Ref. [38]	glucose concentration in tears	graphene-AgNW electrodes	n.a.	0.5 dB/M
Ref. [39]	glucose concentration in saliva	RF-trilayer sensor	0.6 MHz in 1 g L^{-1} of glucose	1 dB for saliva
Ref. [40]	pseudomonas aeruginosa, staphylococcus aureus	Interdigitated capacitor on foil	0.25 MHz per dilutions of concentration	n.a.

Thus, it can be concluded that the PHA-based LC sensor structure can successfully detect different liquids to which the sensor can be exposed, through monitoring the shift in the resonant frequency. The presented sensor can be calibrated using pH meter (we use pH-meter InoLab 720, WTW, Weilheim in Oberbayern, Germany), bearing in mind that two studied media, saliva and gastric acid, differentiate significantly in their pH values. Namely, saliva has pH value between 6.2 and 7.6, whereas gastric juice has acidic pH value in the range from 1 to 2. Additionally, our measured results can be calibrated or confirmed by bulky and costly HPLC or LC/MS instruments. The presented technique based on the wireless principle can find useful application in the biodegradable electronics domain.

4. Conclusions

This work demonstrated the successful implementation of PHA as a low-cost substrate for LC resonant sensors, which would increase the commercial competitiveness of these polymers. A comprehensive structural, morphological and mechanical characterization of the solvent-casted mcl-PHA was performed. The sensor structures were tested in air, and liquid media including artificial saliva and artificial stomach acid. The sensor described in this work, realized on a biodegradable, flexible substrate, can find wide application in the fields of medical diagnostics and biomedical engineering. In the field of biomedicine, biopolymers show many advantages that make them superior to synthetic polymers, predominantly because of their natural origin. In addition, the presented PHA sensor is environmentally friendly, since there are no by-products during the fabrication process or from degradation that would harm water, land, air or living things.

Acknowledgments

Results presented in this article received funding from the EU Horizon 2020 research and innovation programme under the MSC Grant agreement no. 872370—SALSETH, and being partly supported by the project 142-451-2168/2019-02, BP2017 (Bioplastech) and TR32008.

References:

[1] M. Biron, Chapter 2 – The plastics industry: economic overview. In: Biron M, editor. Thermoplastics and thermoplastic composites. 3rd ed. Norwich, NY: William Andrew Publishing (2018) 31–132.

[2] P.R. Rodrigues, D.J. Assis, J.I. Druzian, Simultaneous production of polyhydroxyalkanoate and xanthan gum: From axenic to mixed cultivation, Bioresource Technology 283 (2019) 332–339.

[3] Z. Ali Raza, S. Abid, I.M. Banat, Polyhydroxyalkanoates: Characteristics, production, recent developments and applications, International Biodeterioration & Biodegradation, 126 (2018) 45–56.

[4] M.E. Grigore, R.M. Grigorescu, L. Iancu, R.M. Ion, C. Zaharia, E.R. Andrei, Methods of synthesis, properties and biomedical applications of polyhydroxyalkanoates: a review, Journal of Biomaterials Science, Polymer Edition, (2019) DOI: 10.1080/09205063.2019.1605866.

[5] B. Hazer, A. Steinbuchel, Increased diversification of polyhydroxyalkanoates by modification reactions for industrial and medical applications, Appl Microbiol Biotechnol. 74 (2007) 1–12.
[6] S. Ray, V.C. Kalia, Biomedical applications of polyhydroxyalkanoates, Indian J Microbiol. 57 (2017) 261–269.
[7] K. Luef, F. Stelzer, F. Wiesbrock, Poly (hydroxy alkanoate) s in medical applications. Chem Biochem Eng Q. 29 (2015) 287–297.
[8] A.N. Boyandin, S.V. Prudnikova, V.A. Karpov, V.N. Ivonin, N.L. Do, T.H. Nguyen, T.M.H. Le, N.L. Filichev, A.L. Levin, M.L. Filipenko, T.G. Volova, I.I. Gitelson, Microbial degradation of polyhydroxyalkanoates in tropical soils. Int. Biodeterior. Biodegr. 83 (2013) 77–84.
[9] A. Larrañaga, J. Fernández, A. Vega, A. Etzeberria, C. Ronchel, J.L. Adrio, J.R. Sarasua, Crystallization and its effect on the mechanical properties of a medium chain length polyhydroxyalkanoate, J. Mech. Behav. Biomed. Mater. 39 (2014) 87–94.
[10] S. Philip, T. Keshavarz, I. Roy, Polyhydroxyalkanoates: biodegradable polymers with a range of applications, J. Chem. Technol. Biotechnol. 82 (2007) 233–247.
[11] K. Jia, R. Cao, D. Hua, P. Li, Study of class I and class III polyhydroxyalkanoate (PHA) synthases with substrates containing a modified side chain, Biomacromolecules 17 (4) (2016) 1477–1485.
[12] A. Anjum, M. Zuber, K. Zia, A. Noreen, M. Anjum, S. Tabasum, Microbial production of polyhydroxyalkanoates (PHAs) and its copolymers: a review of recent advancements, Int. J. Biol. Macromol. 89 (2016) 161–174.
[13] V. Urtuvia, P. Villegas, S. Fuentes, M. González, M. Seeger, Burkholderia xenovorans LB400 possesses a functional polyhydroxyalkanoate anabolic pathway encoded by the pha genes and synthesizes poly(3-hydroxybutyrate) under nitrogen-limiting conditions, Int. Microbiol. 21 (1–2) (2018) 47–57.
[14] E. Bugnicourt, P. Cinelli, A. Lazzeri, V. Alvarez, Polyhydroxyalkanoate (PHA): review of synthesis, characteristics, processing and potential applications in packaging. Express Polym. Lett. 8, (2014) 791–808.
[15] C. Sanhueza, F. Acevedo, S. Rocha, P. Villegas, M. Seeger, R. Navia, Polyhydroxyalkanoates as biomaterial for electrospun scaffolds, International Journal of Biological Macromolecules 124 (2019) 102–110.
[16] Z.A. Raza, S. Riaz, I.M. Banat, Polyhydroxyalkanoates: properties and chemical modification approaches for their functionalization. Biotechnol Progress. 34 (2018) 29–41.
[17] L. Gong, D.B. Chase, I. Noda, J. Liu, D.C. Martin, C. Ni, J.F. Rabolt, Discovery of β-form crystal structure in electrospun poly[(R)-3-hydroxybutyrate-co-(R)-3-hydroxyhexanoate] (PHBHx) nanofibers: from fiber mats to single fibers, Macromolecules 48 (17) (2015) 6197–6205.
[18] D. Kim, H. Kim, M. Chung, Y. Rhee, Biosynthesis, modification, and biodegradation of bacterial medium-chain-length polyhydroxyalkanoates, J. Microbiol. 45 (2) (2007) 87–97.
[19] T. Volova, D. Goncharov, A. Sukovatyi, A. Shabanov, E. Nikolaeva, E. Shishatskaya, Electrospinning of polyhydroxyalkanoate fibrous scaffolds: effects on electrospinning parameters on structure and properties, J. Biomater. Sci. Polym. Ed. 25 (4) (2014) 370–393.
[20] M. Zhu,W. Zuo, H. Yu,W. Yang, Y. Chen, Superhydrophobic surface directly created by electrospinning based on hydrophilic material, J. Mater. Sci. 41 (12) (2006) 3793–3797.
[21] M. Xiang, L. Xinjian, X. Han, L. Genxi, Direct electrochemistry and electrocatalysis of hemoglobin in poly-3-hydroxybutyrate membrane, Biosensors and Bioelectronics, 20 (9) (2005) 1836–1842.
[22] X. Ma, R. Yang, G. Li, Hydrogen Peroxide Biosensor Based on the Direct Electrochemistry of Myoglobin Immobilized in Poly-3-Hydroxybutyrate Film, Am. J. Biochem. Biotechnol. 1 (2005) 43–46.

[23] P. Phukon, K. Radhapyari, B. K. Konwar, R. Khan, Natural polyhydroxyalkanoate–gold nanocomposite based biosensor for detection of antimalarial drug artemisinin, Materials Science and Engineering: C, 37 (2014) 314–320.
[24] R. Davis, G. Duane, S.T. Kenny, F. Cerrone, M.W. Guzik, R.P. Babu, E. Casey, K.E. O'Connor, High cell density cultivation of *Pseudomonas putida* KT2440 using glucose without the need for oxygen enriched air supply, Biotechnol. Bioeng. 112 (4) (2015) 725–733.
[25] Y. Elbahloul, A. Steinbüchel, Large-scale production of poly(3-hydroxyoctanoic acid) by Pseudomonas putida GPo1 and a simplified downstream process. Appl. Environ. Microbiol. 75 (3) (2009) 643–651.
[26] X. Pan, J. Li, R. Gun, X. Hu, Preparation and in Vitro Evaluation of Enteric-coated Tablets of Rosiglutazone sodium. Saudi Pharmaceutical Journal 23 (2015) 581–586.
[27] A. Rodriguez-Contreras, Recent Advances in the Use of Polyhydroyalkanoates in Biomedicine; Bioengineering, 6 (2019) 82.
[28] J. Limb, M. You, J. Li, Z. Li, Emerging bone tissue engineering via Polyhydroxyalkanoate (PHA)-based scaffolds, Materials Science and Engineering: C, 79 (2017) 917–929.
[29] B.Y. Yu, C.R. Chen, Y.M. Sun, T.H. Young, The response of rat cerebellar granule neurons (rCGNs) to various polyhydroxyalkanoate (PHA) films, Desalination 245 (2009) 639–646
[30] K. Sofinska, J. Barbasz, T. Witko, J. Dryzek, K. Haraźna, M. Witko, J. Krysciak-Czerwenka, M. Guzik, Structural, topographical, and mechanical characteristics of purified polyhydroxyoctanoate polymer, J. Appl. Polym. Sci. 2019.
[31] A. Benken, Y. Gianchandani, Passive Wireless Pressure Sensing for Gastric Manometry, Micromachines 10 (2019), 868–646.
[32] S. Saremi-Yarahmadi, O. H. Murphy, C. Toumazou, RF Inductive Sensors for Detection of Change in the Ionic Strength and pH of Liquid Samples, Proc. of 2010 IEEE International Symposium on Circuits and Systems, 30 May-2 June 2010, Paris, France, doi: 10.1109/ISCAS.2010.5536953.
[33] M. Dautta, M. Alshetaiwi, J. Escobar, P. Tseng, Passive and wireless, implantable glucose sensing with phenylboronic acid hydrogel-interlayer RF resonators, Biosensors and Bioelectronics 151 (2020) 112004.
[34] M.S. Arefin, M.B. Coskun, T. Alan, J.M. Redoute, A. Neild, M.R. Yuce, A microfabricated fringing field capacitive pH sensor with an integrated readout circuit, Appl. Phys. Lett. 104, (2014) 223503.
[35] G. Crupi, X. Bao, O. J. Babarinde, D. M. M.-P. Schreurs, B. Nauwelaers, Biosensor using a one-port interdigital capacitor: A resonance-based investigation of the permittivity sensitivity for microfluidic broadband bioelectronics applications, Electronics, 9 (2020), 340
[36] N. K. Tiwari, S. P. Singh, D. Mondal, M. Jaleel Akhtar, Flexible biomedical RF sensors to quantify the purity of medical grade glycerol and glucose concentrations, International Journal of Microwave and Wireless Technologies (2019) 1–11.
[37] S. Kim, J. Kim, A. Babajanyan, K. Lee, B. Friedman, Noncontact characterization of glucose by a waveguide microwave probe, Current Applied Physics 9 (2009) 856–860.
[38] J. Kim, M. Kim, M. S. Lee, K. Kim, S. Ji, Y. T. Kim, J. Park, K. Na, K. H. Bae, H. K. Kim, F. Bien, C. Y. Lee, J. U. Park, Wearable smart sensor systems integrated on soft contact lenses for wireless ocular diagnostics, Nature communication, 8 (2016) 14997.
[39] P. Tseng, B. Napier, L. Garbarini, D. L. Kaplan, F. G. Omenetto, Functional, RF-Trilayer Sensors for Tooth-Mounted, Wireless Monitoring of the Oral Cavity and Food Consumption, Adv. Mater. (2018), 1703257.
[40] T. Kojić, M. Radovanović, G. Stojanović, B. Pivaš, D. Medić, H. Al-Salami, Comparison of performances of flexible sensors on foil and paper for efficient bacterial concentration measurement, Sensor Review, 40 (2020) 1–7.

Figure captions:

Figure 1. (a) Visual appearance of the processed PHA sample, (b) SEM micrograph of the sample at ×200 magnification, (c) SEM micrograph of the sample cross-section at ×250 magnification

Figure 2. (a) 2D profilometer image of surface structure of sample; (b) 3D profilometer image of sample

Figure 3. Three-dimensional AFM images of PHA sample topography obtained for two scanning areas: (a) 50 μm × 50 μm and (b) 5 μm × 5 μm

Figure 4. 2D AFM images showing topography ((a) and (c)) and LFM signal ((b) and (d)) for the scanned areas 50 μm × 50 μm and 5 μm × 5 μm

Figure 5. (a) Detail of the user interface of ImageJ software during the measurement of the contact angle (b) Graphical representation of contact angle results for a drop of distilled water

Figure 6. Load-displacement curves for three analyzed cases

Figure 7. LC resonant structure: (a) manufactured from PHA, (b) after gold coating

Figure 8. Sensor appearance when there is artificial saliva between the capacitor electrodes

Figure 9. Frequency dependence of amplitude of S11 parameters in three chosen media

Figure 10. Variation of the resonant frequency depending on the type of the medium

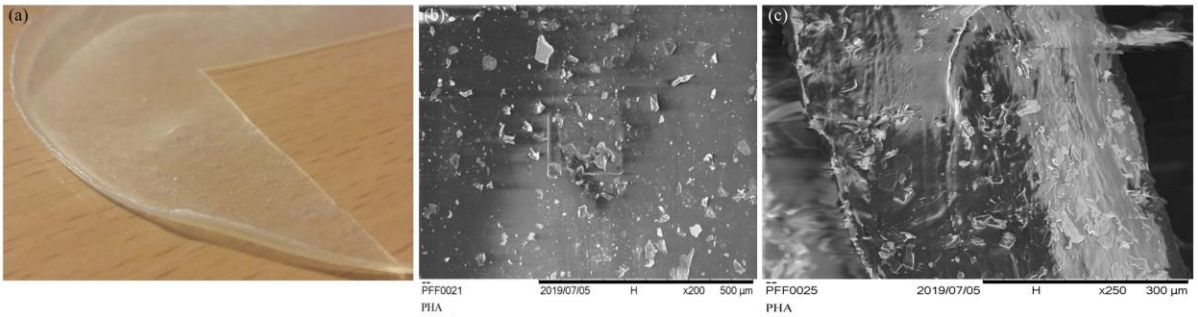

473

474

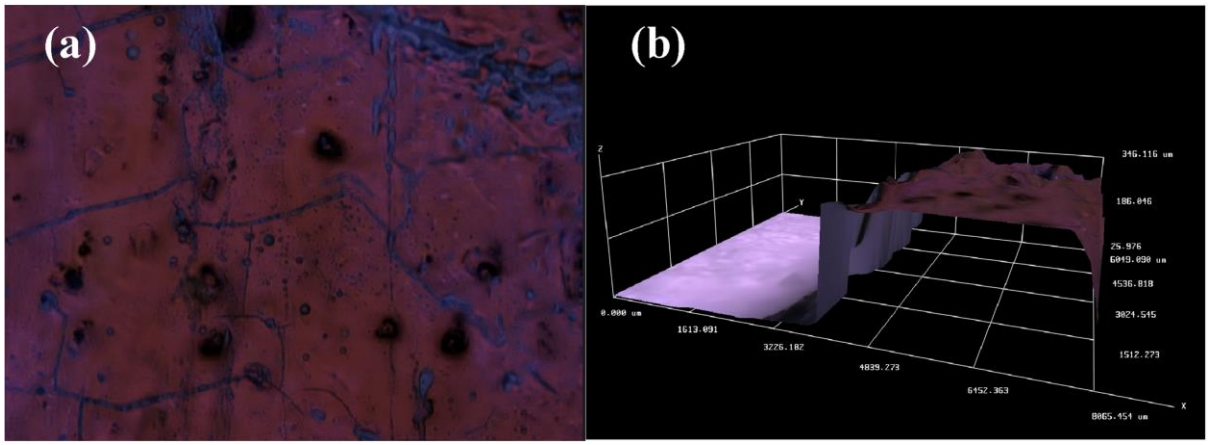

475

476

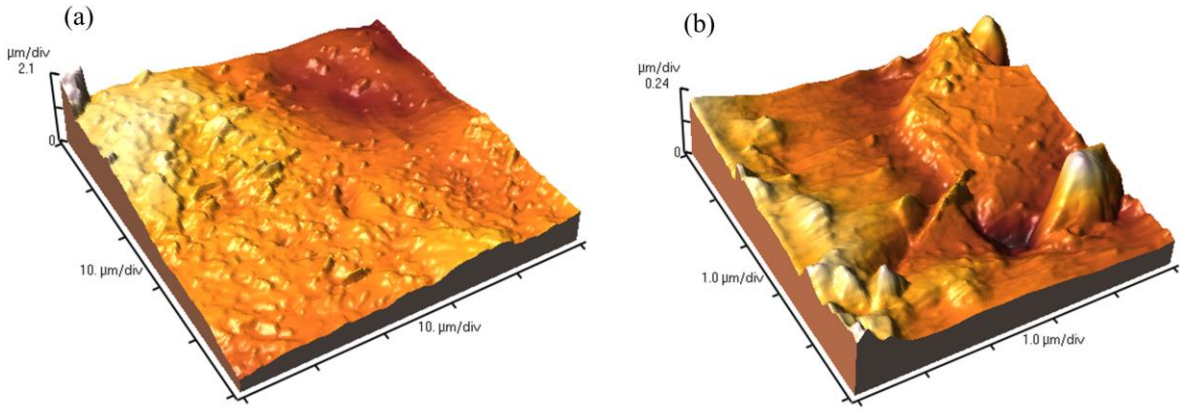

477

478

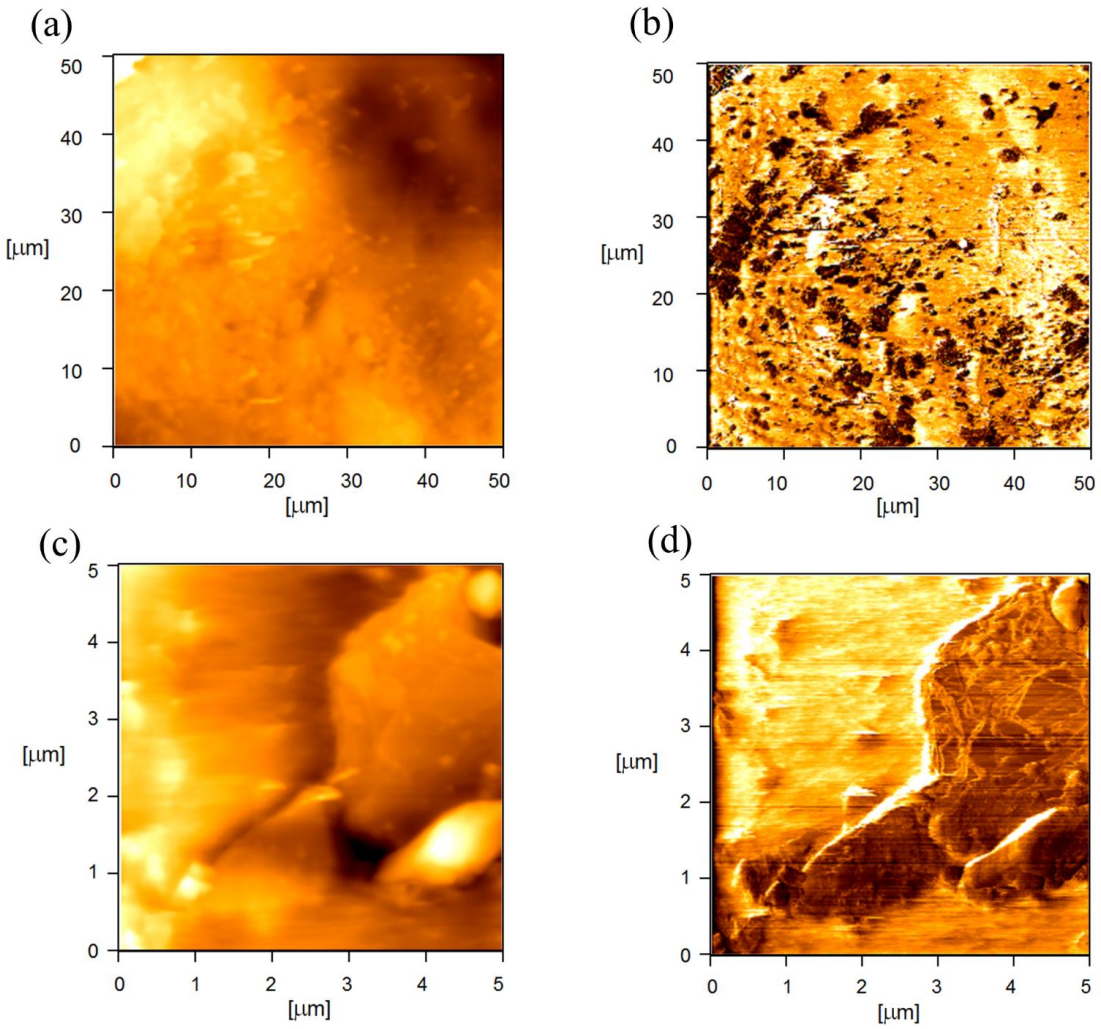
(a)
(b)
(c)
(d)
[μm]
0
10
20
30
40
50
1
2
3
4
5

479

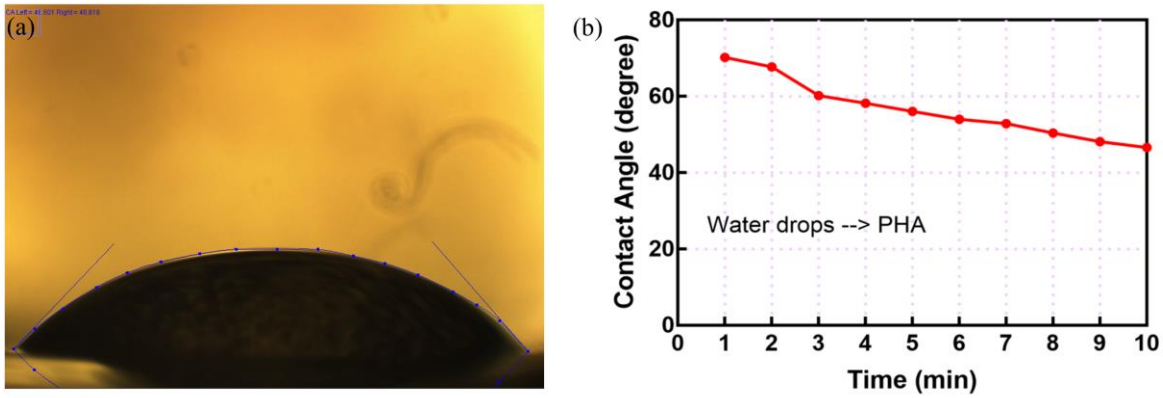
(a)
(b)
Contact Angle (degree)
Time (min)
Water drops --> PHA
0
20
40
60
80
1
2
3
4
5
6
7
8
9
10

480

481

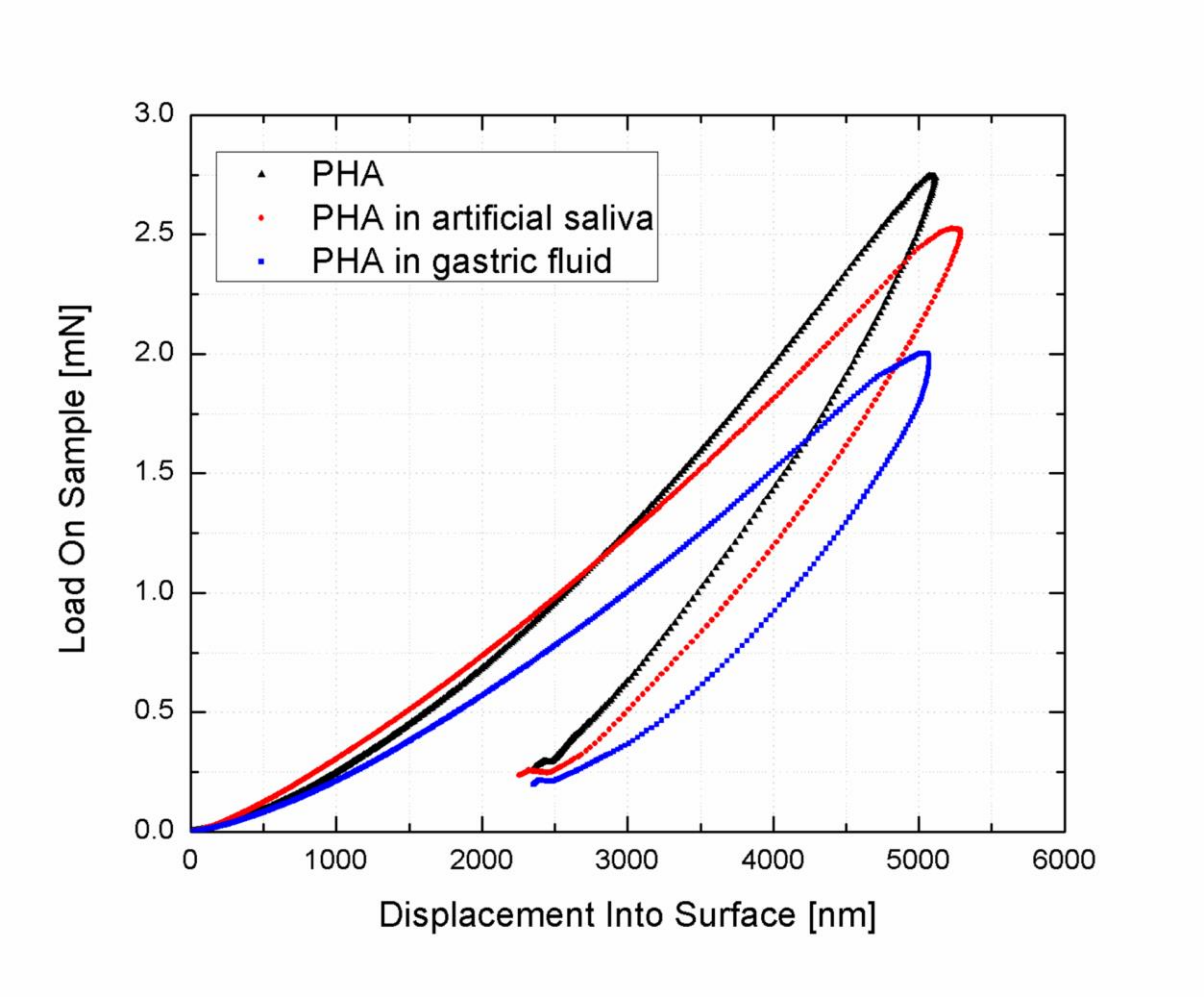
PHA
PHA in artificial saliva
PHA in gastric fluid
Load On Sample [mN]
Displacement Into Surface [nm]
3.0
2.5
2.0
1.5
1.0
0.5
0.0
0
1000
2000
3000
4000
5000
6000

482

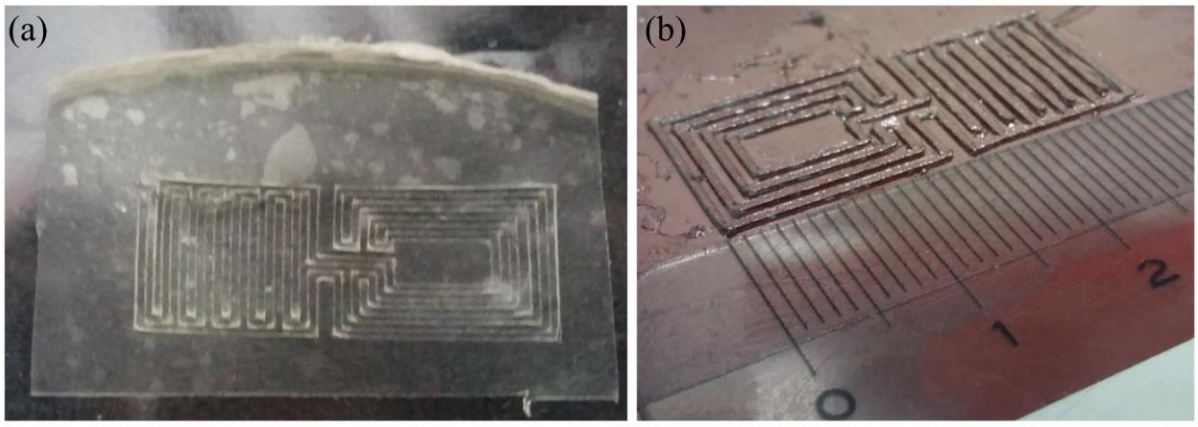
(a)
(b)

483

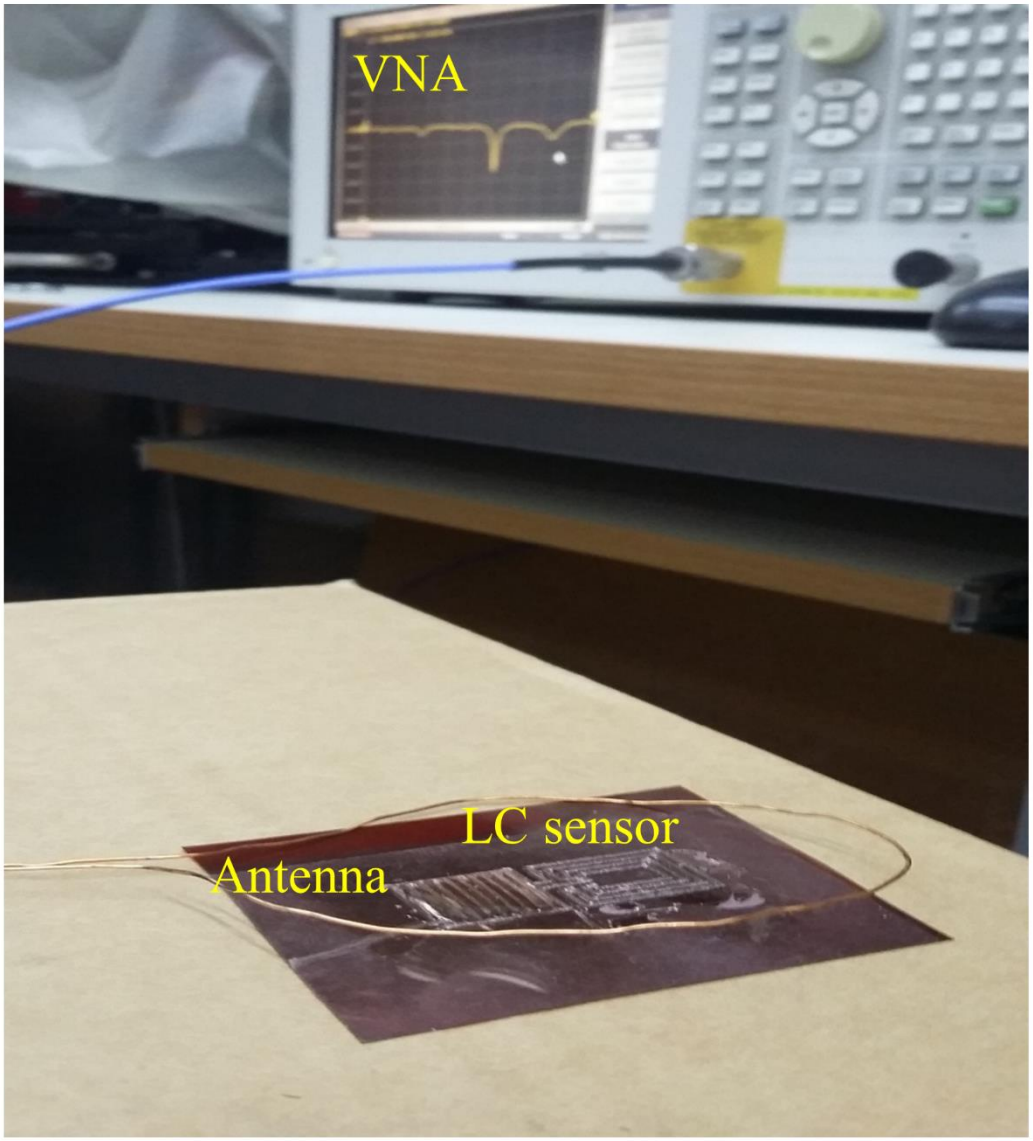
VNA
LC sensor
Antenna

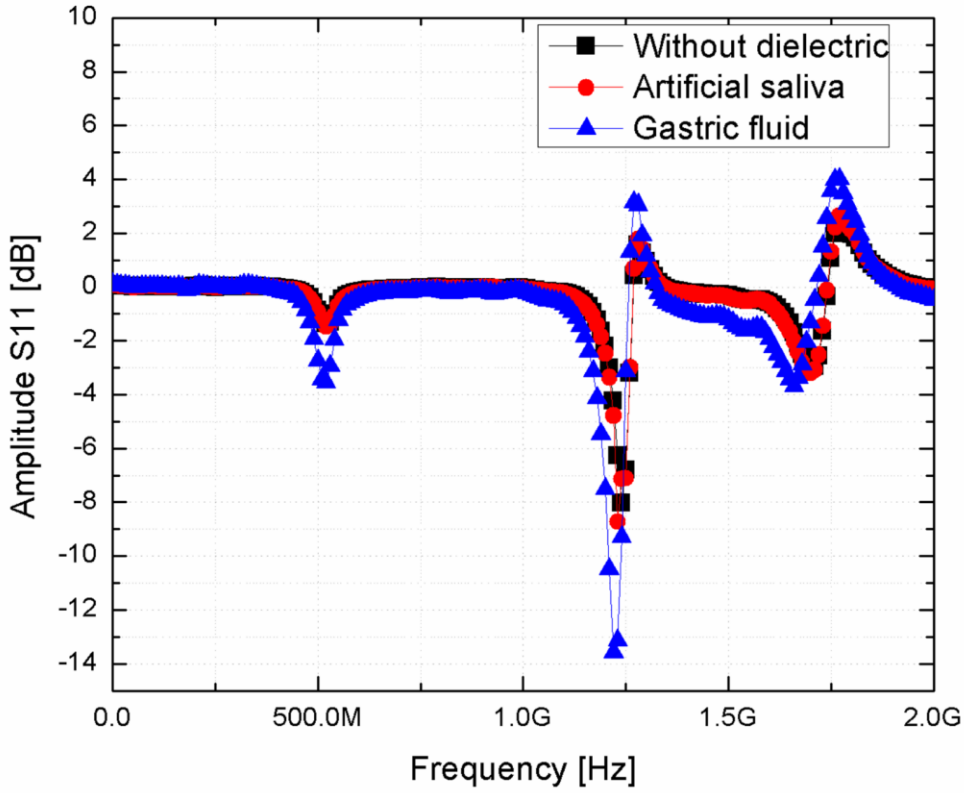
Without dielectric
Artificial saliva
Gastric fluid
Amplitude S11 [dB]
Frequency [Hz]
10
8
6
4
2
0
-2
-4
-6
-8
-10
-12
-14
0.0
500.0M
1.0G
1.5G
2.0G

485

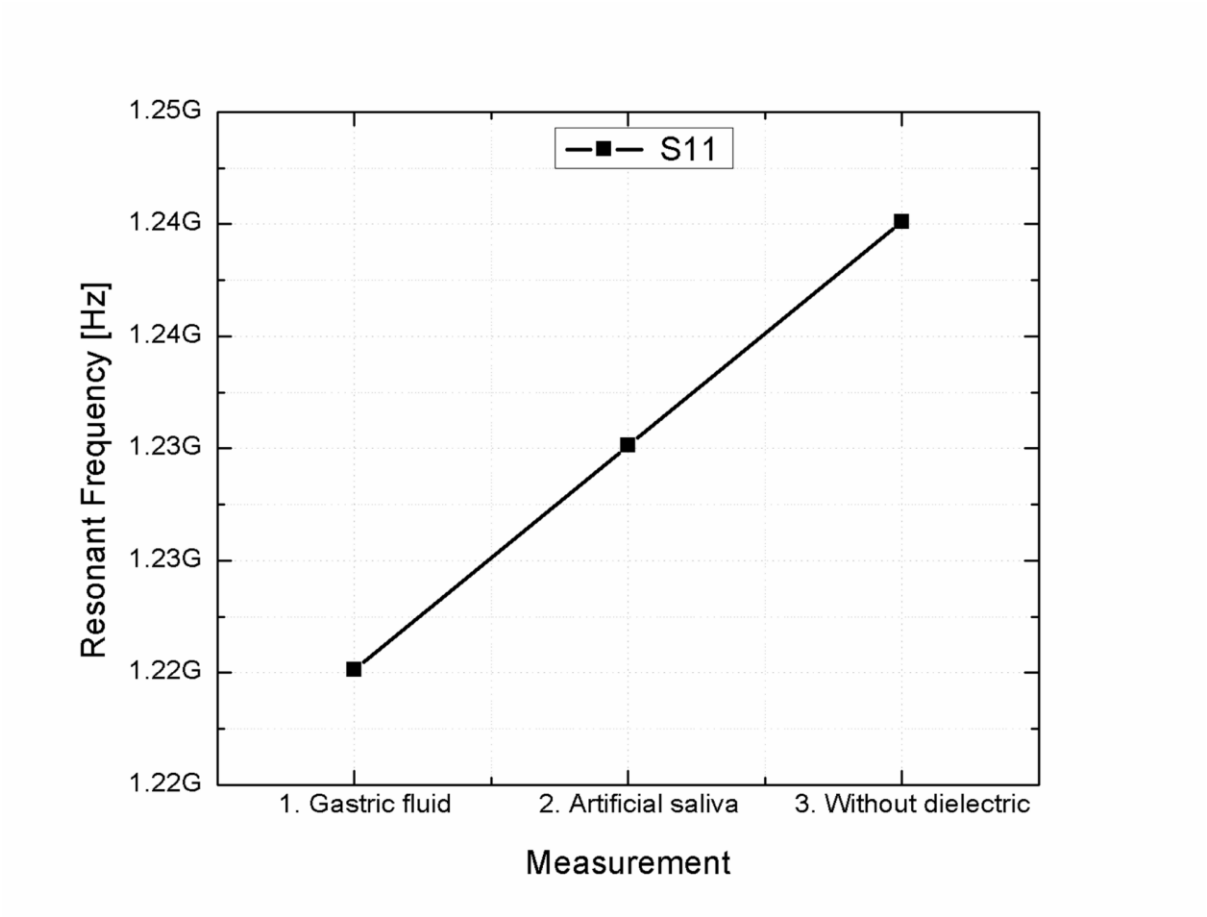
S11
Resonant Frequency [Hz]
1.25G
1.24G
1.24G
1.23G
1.23G
1.22G
1.22G
1. Gastric fluid
2. Artificial saliva
3. Without dielectric
Measurement

486

487